JOURNAL OF APPLIED ELECTROCHEMISTRY **26** (1996) 1273–1277

Effect of cysteine on the kinetics of electroless nickel deposition

K. P. HAN*, J. L. FANG

**Department of Chemistry, Applied Chemistry Institute, Nanjing University, Nanjing 210093 People's Republic of China*

Received 29 September 1995; revised 16 January 1996

Cysteine is found to accelerate electroless nickel (EN) deposition and hydrogen evolution simultaneously. Changes in the activation energy of the EN reaction and the electrochemical behaviour of the EN bath due to the presence of cysteine were studied. The composition of the deposit formed was determined by XPS. The results show that the activation energy of the EN reaction is decreased when cysteine is added to the bath, and also that cysteine only influences the anodic process and has no direct effect on the cathodic process. The high resolution XPS spectra show that cysteine is adsorbed in the surface layer, and S^{2-} in the inner layer of the deposit. It is deduced that cysteine may participate in the formation of a reactive intermediate and facilitate the oxidation of $H_2PO_2^-$, which results in the acceleration of EN plating.

1. Introduction

Since the discovery of electroless nickel plating in 1944 by Brenner and Riddell [1], this plating technique has been extensively used in the electronics, automobile, aerospace and other industries. Frequently the rate of electroless nickel plating with hypophosphite as reducing agent is below $20\,\mu m\,h^{-1}$, so that work on increasing the deposition rate and clarifying the acceleration mechanism is of great importance in both practice and theory.

It has been found that thiourea and other sulfur-containing compounds, such as thiocyanate, can increase the rate of nickel deposition when present in very small concentration [2]. As reported by Gutzeit [3], sodium or potassium salts of mono- and dibasic organic acids, which were originally buffers in EN baths, also caused enhancement of the deposition rate. Fang [4] has pointed out that the simultaneous employment of two different complexing agents can form a mixed ligand complex which improves the transmission of electrons and increases the nickel deposition rate. In addition, glycine [5] has also been found to exhibit an accelerating effect. Radiochemical studies of thiourea in electroless nickel deposition have been conducted by Kivel and Sallo [6]. However, there has been no published study on the acceleration effect of cysteine on electroless nickel deposition.

This paper describes the effect of cysteine on the rate of nickel deposition and hydrogen evolution, activation energy of the EN reaction, partial cathodic and anodic polarization curves and steady state potential. The composition of the deposit formed with addition of cysteine was also determined by XPS. A possible mechanism was proposed to account for the findings.

2. Experimental details

Iron specimens, 2 cm × 5 cm × 0.2 cm, were polished with a fine grit paper, degreased and activated in dilute hydrochloric acid solution. The washed specimens were then introduced to the electroless nickel plating bath. The essential composition of the solutions was $35\,g\,dm^{-3}$ $NiSO_4 \cdot 7H_2O$, $25\,g\,dm^{-3}$ $NaH_2PO_2 \cdot H_2O$, $15\,g\,dm^{-3}$ sodium citrate, $5\,g\,dm^{-3}$ succinic acid, $1.5 \times 10^{-3}\,g\,dm^{-3}$ lead acetate, pH 5.8. Bath temperatures were controlled at $90 \pm 0.5\,^{\circ}C$. All chemicals used in preparing the plating solutions were reagent grade. No agitation was provided during the plating.

The determination of nickel deposition rate was described in our earlier work [7]. The method for hydrogen evolution determination is described in [8]. Electrochemical measurements were conducted with an EG&G Princeton Applied Research Potentiostat/Galvanostat Model 273. The working electrode was a $1\,cm^2$ iron sheet which had been freshly plated with nickel. The counter electrode was a $4\,cm^2$ platinum sheet, and a saturated calomel electrode (SCE) was used as reference. Linear scanning voltammetry (LSV) was used to plot cathodic and anodic polarization curves. The scan rate was $1\,mV\,s^{-1}$. A Perkin–Elmer PHI 550 ESCA/SAM electron spectrometer [9] with AlK_α X-ray anode (1486.6 eV) was employed for the deposit surface analysis. The pass energy was 50 eV for high resolution XPS spectrum measurements.

3. Results

3.1. *Nickel deposition and hydrogen evolution rate*

The variations in the nickel deposition rate and hydrogen evolution rate with cysteine concentration

---

* Author to whom correspondence should be addressed.

0021-891X

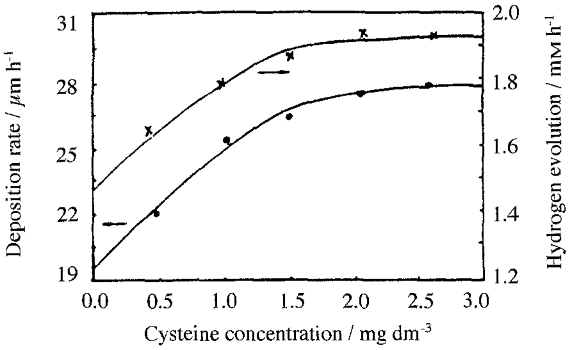

Fig. 1. Variation of the rate of nickel deposition and hydrogen evolution with cysteine concentration.

are shown in Fig. 1. A rapid increase in the nickel deposition and hydrogen evolution rate is observed. At cysteine concentrations greater than 2 mg dm^{-3}, both curves reach a constant value. These suggest that the nickel deposition and hydrogen evolution reactions are accelerated simultaneously by cysteine.

3.2. *Activation energy*

It is well known that the relationship between reaction rate V and the activation energy E_a of an EN reaction can be expressed as follows:

$$\log V = \log a - \frac{E_a}{2.3\,RT} \qquad (1)$$

From the slope D of the $\log V/T^{-1}$ straight line, the activation energy E_a can be calculated according to the following formula:

$$E_a = -2.3\,RD \qquad (2)$$

where R is the gas constant.

From the $\log V/T^{-1}$ curves of Fig. 2, the activation energies with and without addition of 2 mg dm^{-3} of cysteine are 52.3 and 68.5 kJ mol^{-1}, respectively. Thus the presence of cysteine decreases the activation energy of EN.

3.3. *Partial polarization curves*

According to the mixed potential theory [10], the electroless plating of metal can be considered as the anodic oxidation of the reducing agent and the cathodic deposition of the metal. Following this concept, Haruyama *et al.* [11] estimated the rate of electroless plating of cobalt by the partial polarization curves in the bath removing either NaH_2PO_2 or $CoSO_4$ from the standard bath composition in their work. The same polarization method was also utilized to study the effect of various concentrations of metal ions and reducing agents at different pH values on electroless copper deposition by Hung and Ohno [12].

It is generally accepted that the overall reaction in EN plating consists of two kinds of simultaneous reactions [13]:

(i) the cathodic reaction of Ni^{2+}, H^+ and $H_2PO_2^-$ or the deposition of Ni–P alloy and the production of hydrogen, that is,

$$Ni^{2+} + 2e^- \longrightarrow Ni \qquad (3)$$

$$2H^+ + 2e^- \longrightarrow H_2 \qquad (4)$$

$$H_2PO_2^- + 2H^+ + e^- \longrightarrow P + 2H_2O \qquad (5)$$

(ii) the anodic oxidation of $H_2PO_2^-$, that is,

$$H_2PO_2^- + H_2O \longrightarrow H_2PO_3^- + H + H^+ + e^- \qquad (6)$$

To develop current–potential curves for the partial cathodic reaction, solutions containing nickel sulfate, sodium citrate, succinic acid and lead acetate were employed. Hypophosphite was not included in the solutions and different amounts of cysteine were added to the solutions. The current–potential curves

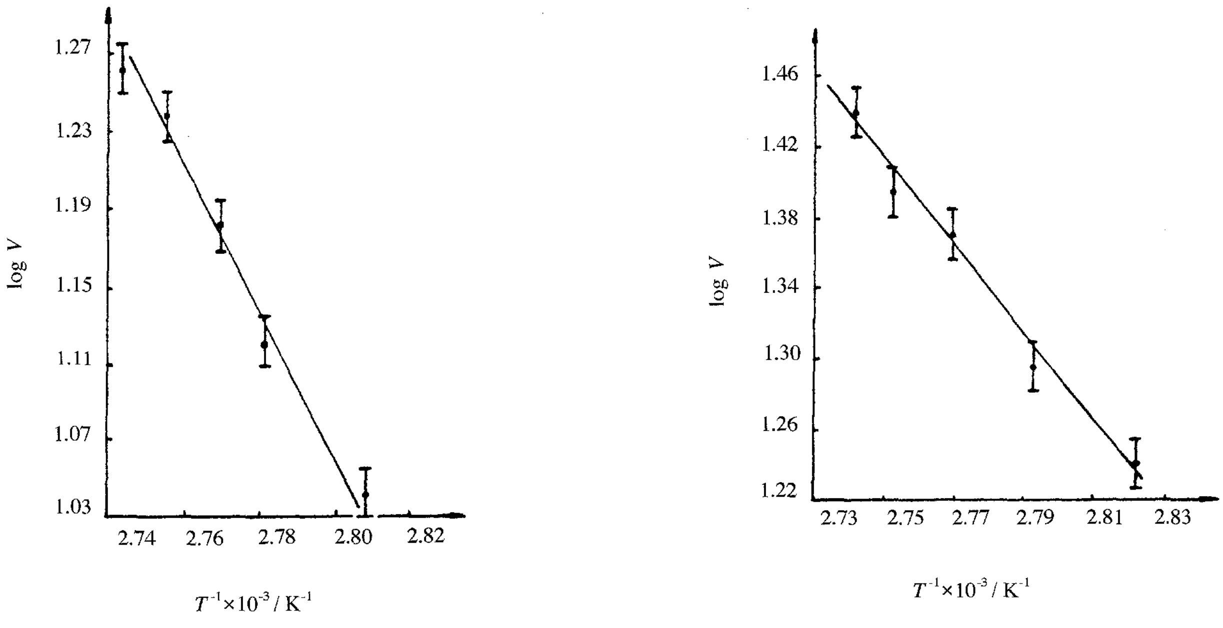

(a) (b)

Fig. 2. The $\log V/T^{-1}$ curves of EN reaction. (a) Bath without cysteine, (b) bath with 2 mg dm^{-3} cysteine.

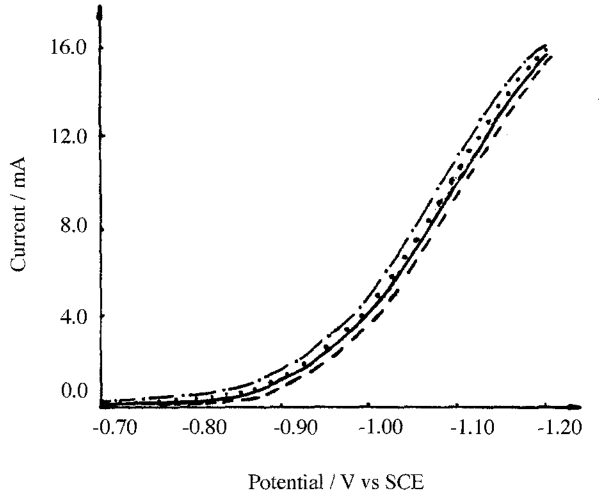

Fig. 3. Cathodic polarization curves of EN plating bath without $H_2PO_2^-$, scan rate: 1 mV s^{-1}, pH 5.8, temp.: 90 ± 0.5 °C. Cysteine concentration: (——) 0; (···) 1; (– – –) 2; (–·–·) 3.

obtained at a scan rate of 1 mV s^{-1} are shown in Fig. 3. It can be seen that the cathodic polarization curves at different cysteine concentrations are broadly similar. This demonstrates little influence of cysteine on the cathodic process in the absence of $H_2PO_2^-$.

To develop current–potential curves for the partial anodic reaction, solutions containing hypophosphite, sodium citrate, succinic acid and lead acetate were formulated. Nickel ions were not employed in the solutions and different concentrations of cysteine were added to the solutions. The current–potential curves recorded at 1 mV s^{-1} are shown in Fig. 4. The oxidation current of $H_2PO_2^-$ increases with increase in cysteine concentration and the anodic potential shifts positively. This indicates that cysteine is an anodic depolarizer and accelerates the oxidation of $H_2PO_2^-$.

3.4. *Steady state potential*

EN deposition reaction may proceed spontaneously for some metals; these metals are known as catalytic metals. Fang [14] has proposed that the steady state potential of metals provides a simple parameter for estimating the catalytic activity in EN deposition, and that if the steady state potential of the metal is more negative, its reactivity is higher.

It has been reported that accelerators (or inhibitors) can alter the electrochemical parameters at the electrode/solution interface [15]; thus the steady state potential of the bath with different amounts of cysteine added was investigated. The result is shown in Fig. 5. It can be seen that the steady state potential moves in the negative direction leading to a plateau, and that the presence of 2 mg dm^{-3} of cysteine shifts the steady state potential some 300 mV more negative to approximately −331 mV where a considerable acceleration effect is anticipated. It should also be noted that this potential vs. cysteine concentration curve follows the same characteristics as shown in Fig. 1. This result is in good agreement with that obtained by Feldstein and Lancsek [15], who studied the variation of the nickel deposition rate and the steady state potential measured on the nickel surface with sodium formate concentration.

3.5. *XPS analysis of the deposit*

Figure 6 shows the high resolution X-ray photoelectron spectra of sulfur in the deposit before and after Ar^+ sputtering. Before sputtering the dominant peak value (168.9 eV) corresponds to that in $Fe_2(SO_4)_3$ [16], indicating that SO_4^{2-} is adsorbed on the external surface of the deposit. Meanwhile the peak of low valence sulfur occurs at 160 ~ 164 eV [16], suggesting that cysteine may also be adsorbed on the surface of the deposit. Due to the trace amount of cysteine in the EN bath and the rinsing operation of the deposit before the surface analysis, the cysteine peak is weak. After Ar^+ sputtering for 5 min, a new strong peak at 161.7 eV appears, which is close to that of S in Na_2S [11]. At the same time, the intensity of peak at 168.9 eV decreases; this may be related to

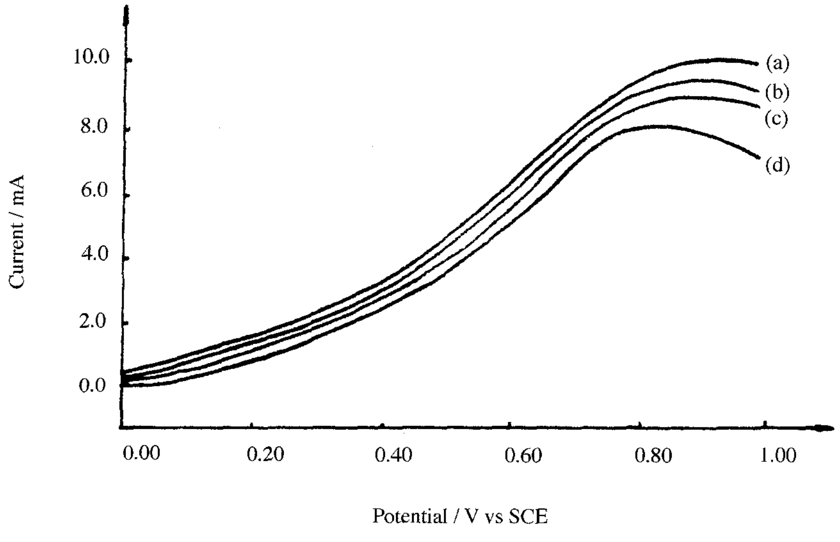

Fig. 4. Anodic polarization curves of EN plating bath in the absence of Ni^{2+}, scan rate: 1 mV s^{-1}, pH 5.8, temp.: 90 ± 0.5 °C. Cysteine concentration: (a) 3; (b) 2; (c) 1; (d) 0.

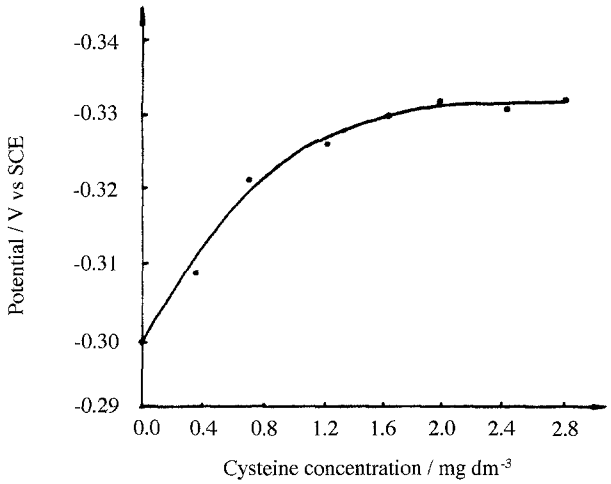

Fig. 5. Variation of the steady state potential with cysteine concentration.

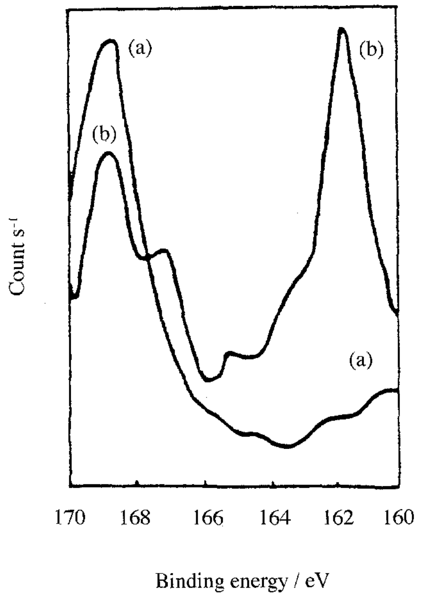

Fig. 6. High resolution XPS spectra of sulfur. (a) No sputtering, (b) sputtering for 5 min.

the inclusion of SO_4^{2-} in the deposit. Therefore it is suggested that sulfur exists in the internal layer of the deposit as S^{2-} and SO_4^{2-}.

4. Discussion

From the above partial polarization curves, it is clear that cysteine accelerates the anodic oxidation of $H_2PO_2^-$ and has no direct effect on the cathodic process. This assumption can be explained by Dimroth's equation [17]:

$$\ln k = \alpha \Delta E + \text{constant} \qquad (7)$$

$$\Delta E = \varphi_a - \varphi_k \qquad (8)$$

where k is the reaction rate constant, α is a constant, φ_a is the anodic potential, φ_k is the cathodic potential, and ΔE is the difference between anodic and cathodic potential.

Equation 7 indicates that k increases exponentially with ΔE. Since cysteine has no effect on φ_k and only affects φ_a, the positive movement of φ_a, as shown in Fig. 4, leads to an increase in ΔE and the subsequent exponential increase in k. Therefore both nickel deposition and hydrogen evolution are accelerated simultaneously. The results of activation energy determination show that cysteine decreases the activation energy of EN reaction, the decrease in the activation energy indicates the formation of the more stable reactive intermediate. Thus it can be inferred that cysteine may be involved in the formation of the reactive intermediate in the EN reaction. The results of XPS analysis, which illustrated that S^{2-} exists in the internal layer of the deposit, are consistent with the radiochemical determination by Kivel and Sallo [6], who reported that the appearance of S^{2-} in the deposit resulted from the reduction of the C–S bond of the thiourea molecule.

In view of the above analyses, it may be concluded that cysteine participates in the formation of the reactive intermediate in the course of EN plating, which facilitates the oxidation of $H_2PO_2^-$ and thereby accelerates the overall EN reaction; meanwhile, some cysteine is reduced to S^{2-}.

A model has been proposed to illustrate the acceleration effect of electroless nickel deposition by cysteine, as shown in Fig. 7. According to the atomic hydrogen theory of EN plating [18], tetrahedral $H_2PO_2^-$ is adsorbed on the catalytic metal surface, since catalytic metal has strong adsorption ability for hydrogen. Cysteine is a soft base, since it has donor atoms which are generally easily polarized and are of low electronegativity. From the general rule of acid–base interaction [19], soft pairs have the greatest tendency to interact. On this basis it may be expected that cysteine interacts with the metal substrate, which may be classified as a soft acid type and, as a consequence, results in adsorption on the

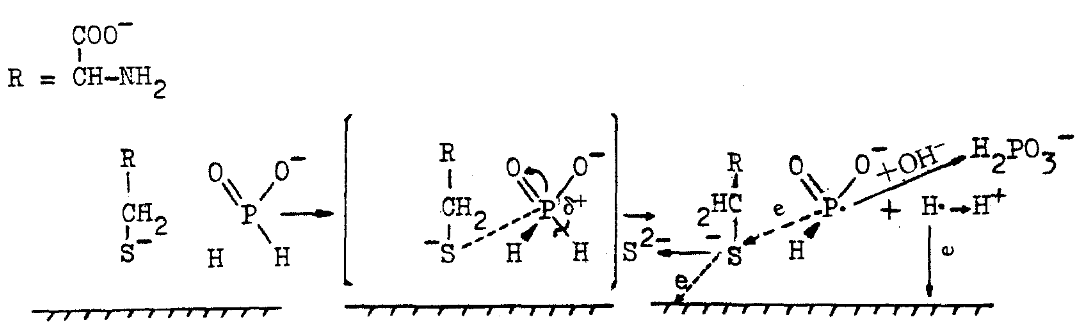

Fig. 7. A proposed model for the acceleration effect by cysteine.

catalytic surface via the sulfur atom, which is the most polarizable and is of the lowest electronegativity.

Due to the higher electronegativity of the oxygen atom, the phosphorus atom of hypophosphite ion is positively charged. It is anticipated that the reactive intermediate of the EN plating is developed through a chemical interaction between the $P^{\delta+}$ of $H_2PO_2^-$ and $S^{\delta-}$ of cysteine, which probably accounts for a weakening of the P–H bond in $H_2PO_2^-$. It follows that the rapid cleavage of the P–H bond in $H_2PO_2^-$ occurs, that is, the oxidation of $H_2PO_2^-$ is accelerated. As the two products of cleavage of the P–H bond in $H_2PO_2^-$, the free radical HPO_2 combines with OH^- derived from the EN solution and thereby produces $H_2PO_3^-$. Meanwhile the hydrogen atom releases electrons and thereby yields H^+, leading to a decrease in the pH of the solution. This explains why the pH of the solution is found to decrease with the evolution of hydrogen during the EN plating process.

On the other hand, it can be postulated that following the cleavage of the P–H bond, the electron on the phosphorus atom may easily be transmitted to the metal surface via the sulfur atom of cysteine due to the good conductivity of the sulfur atom. Because the metal surface obtains more electrons from $H_2PO_2^-$ and atomic H, the surface potential or steady state potential of the metal moves negatively. As shown in Fig. 5, the reactivity of the catalytic metal surface is thus enhanced. Therefore the reduction of Ni^{2+}, or the nickel deposition, is accelerated. Moreover, $H_2PO_2^-$ can be further reduced to elemental phosphorus, which combines with the elemental nickel resulting from the reduction of Ni^{2+}, to form Ni–P alloy. It also should be noted that cysteine may receive some electrons, from the cleavage of the P–H bond in $H_2PO_2^-$; this results in the formation of sulphide, which is more likely to be incorporated in the Ni–P deposit. Thus it is not surprising that S^{2-} exists in the deposit.

5. Conclusion

It is concluded that:

(i) Cysteine is an effective accelerator for the deposition of nickel. The presence of cysteine decreases the activation energy of the EN reaction and shifts the steady state potential of the EN solution in the negative direction.

(ii) The cathodic and anodic polarization curves show that the addition of cysteine accelerates the oxidation of hypophosphite.

(iii) The XPS analysis of the deposit reveals that trace cysteine exists on the deposit surface and S^{2-} in the inner layer of the deposit.

(iv) The acceleration effect of cysteine on electroless nickel deposition may be due to interference in the anodic process.

Acknowledgements

The authors wish to acknowledge the cooperation of State Key Laboratory of Coordination Chemistry, Nanjing University and Modern Analysis Center, Nanjing University for Electrochemical Measurement and Electron Spectroscopy Determination.

References

[1] A. Brenner and G. Riddell, *Proc. AES An. Tech. Conf.* **33** (1946) 16.
[2] C. H. deMinjer and A. Brenner, *Plating* **44** (1957) 1927.
[3] G. Gutzeit, *ibid.* **47** (1960) 63.
[4] J. L. Fang, *Chemistry* **4** (1978) 226.
[5] K. Panker, Amer. Electroplating Society 71st Annual Technical Conference (1984) p. 16.
[6] J. Kivel and J. S. Sallo, *J. Electrochem. Soc.* **112** (1965) 1203.
[7] J. L. Fang, Y. Wu, M. Zhang and J. Fang, *Mater. Protect.* **27** (1994) 1.
[8] A. Hung and I. Ohno, *Plat. Surf. Finish.* **54** (1990) 3.
[9] J. L. Fang and N. J. Wu, *J. Appl. Electrochem.* **20** (1990) 231.
[10] M. Paunovic, *Plating* **55** (1968) 1161.
[11] S. Haruyama, A. Yoshizawa and I. Ohno, *J. Met. Finish. Soc. Jap.* **30** (1979) 289.
[12] A. Hung and I. Ohno, *J. Electrochem. Soc.* **137** (1990) 918.
[13] M. Paunovic, AES 1st Electroless Plating Symposium (1982) p. 2.
[14] J. L. Fang, *Acta Chimica Sinica* **41** (1983) 29.
[15] N. Feldstein and T. S. Lancsek, *J. Electrochem. Soc.* **118** (1971) 869.
[16] C. D. Wagner, W. M. Riggs, L. E. Davis, J. E. Moulder and G. E. Muilenberg, 'Handbook of X-ray Photoelectron Spectroscopy', Perkin-Elmer Corp., Eden Frairie Minnesota (1978).
[17] D. Dimroth, *Angew. Chem.* **46** (1933) 57.
[18] R. M. Lukes, *Plating* **51** (1964) 69.
[19] R. G. Pearson, *J. Chem. Educ.* **45** (1968) 581.